Magnetic ordering of Nd^{3+} in single-crystal $NdBa_2Cu_3O_{6+x}$

A. T. Boothroyd and J. M. Reynolds
Clarendon Laboratory, Oxford University, Oxford OX1 3PU, United Kingdom

N. H. Andersen
Condensed Matter Physics and Chemistry Department, Risø National Laboratory, DK-4000 Roskilde, Denmark

E. Brecht and Th. Wolf
Forschungszentrum Karlsruhe, INFP and ITP, D-76021 Karlsruhe, Germany

A. J. S. Chowdhury
Clarendon Laboratory, Oxford University, Oxford OX1 3PU, United Kingdom
(Received 24 February 1999)

We describe a neutron-diffraction study of the low-temperature magnetic ordering in single crystals of $NdBa_2Cu_3O_{6+x}$. We investigated a superconducting crystal ($T_c = 95.5$ K), and two nonsuperconducting crystals ($x \approx 0.1$). The two nonsuperconducting crystals differed in their Cu sublattice magnetic ordering. One (*A*) exhibited the simple AFI antiferromagnetic spin structure down to the lowest attainable temperature (0.3 K), while the other (*B*) began to reorder into the AFII phase below 30 K. We observed long-range antiferromagnetic ordering of the Nd sublattice in all three crystals, but in crystal *B* the Nd ordering was of very short range in the *c* direction. The onset of Nd ordering produced no detectable changes in the Cu ordering in the nonsuperconducting crystals, and from this we place an upper limit of 0.05 meV on the strength of any Nd-Cu pseudodipolar magnetic coupling. The ordered arrangements of the Nd moments refined from the diffraction intensities agree broadly with those deduced previously from neutron powder diffraction studies, but differ in some of the details. [S0163-1829(99)02826-X]

I. INTRODUCTION

Rare-earth magnetic ordering is a common feature of the layered copper oxide superconductors, and has been investigated extensively in the $RBa_2Cu_3O_{6+x}$ series (R = rare earth) of compounds.[1] With the exception of $PrBa_2Cu_3O_{6+x}$,[2] this magnetism occurs at low temperatures ($T_R \leqslant 2$ K), coexists with superconductivity, and does not play any major role in the formation of the superconducting state.

While not a threat to superconductivity (apart from Pr), the magnetic rare-earth ions do nevertheless have some contact with the electronic states on the CuO_2 planes, and the existence of this interaction is both interesting and useful. For the light rare earths in particular, T_R is too large for the ordering to be caused solely by dipole forces, and some form of weak exchange coupling via orbitals on the planes is implied. One effect of this coupling is to render the rare-earth ions as essentially passive observers of the events taking place in the superconducting layers. Thus, for example, measurements of the relaxation of crystal-field transitions of Tm^{3+} (Ref. 3) and Ho^{3+} (Ref. 4) ions lightly doped into $YBa_2Cu_3O_{6+x}$ (YBCO) have revealed important information about the anisotropy of the superconducting order parameter and about pseudogap formation above T_c. Mössbauer spectroscopy[5] and nuclear magnetic resonance spectroscopy[6] are other techniques that have been used to observe the Cu spin dynamics from a vantage point on the rare-earth site.

The work reported in this paper addresses the general problem of the interplay between R and Cu magnetism in $RBa_2Cu_3O_{6+x}$, and was stimulated in particular by recent observations of the Pr magnetic ordering in $PrBa_2Cu_3O_{6+x}$.[7–9] As noted above, the Pr member of the $RBa_2Cu_3O_{6+x}$ series is anomalous in that conventionally prepared samples do not superconduct for any x.[2,10] It is also exceptional in its magnetic properties, displaying Cu antiferromagnetism at temperatures in the vicinity of room temperature, even when fully doped ($x \approx 1$),[11] and Pr ordering below $T_{Pr} = 11-17$ K for $x = 0-1$.[12] The most recent studies have revealed a magnetic coupling between the Pr and Cu sublattices substantial enough to drive the Cu spins into a noncollinear arrangement below T_{Pr}.[7] This magnetic phase, which we refer to as AFIII, is consistent with the symmetry of a pseudodipolar interaction[13] (i.e., the reorientation is mediated by the off-diagonal terms in the Pr-Cu exchange tensor). A similar type of coupling has been postulated to explain the magnetic transitions in R_2CuO_4.[14] If such an R-Cu interaction were present in the other $RBa_2Cu_3O_{6+x}$ compounds then it could have important implications for the interpretation of R-site relaxation measurements that probe the local dynamic susceptibility $\chi(\mathbf{q},\omega)$ of the CuO_2 planes.[3–6] This is because the off-diagonal terms in the exchange tensor couple the R site most strongly to wave vectors around $\mathbf{q} = (\pi/a, \pi/b)$ in the Cu spin-fluctuation spectrum, whereas the diagonal terms preferentially transmit fluctuations close to $\mathbf{q} = (0,0)$.[13] An R-Cu pseudodipolar interaction would also account for the detection of a Cu-derived molecular field at the Y site in $YBa_2Cu_3O_{6+x}$ by ^{170}Yb Mössbauer spectroscopy.[5]

One of the aims of the present investigation, therefore, was to find out whether a pseudodipolar type of R-Cu cou-

pling could be detected in other $R Ba_2Cu_3O_{6+x}$ compounds that do not display such anomalous properties as $PrBa_2Cu_3O_{6+x}$. The strategy was to search for evidence of a linkage between the magnetic ordering of the R and Cu sublattices. We chose $R=$Nd for this study because it is known that the magnetic ordering of the Nd sublattice occurs at considerably higher temperatures than could be produced solely by magnetic dipole interactions between the saturated Nd moments of $\sim 1\mu_B$.[15] Furthermore, the Nd ordering temperature shows a significant variation with doping, changing from $T_{Nd} \approx 0.6$ K at $x \approx 1$ to $T_{Nd} \approx 1.7$ K at $x \approx 0$,[16] and this suggests that the antiferromagnetic ordering of the Cu sublattice in underdoped samples may have an effect on the Nd ordering. By contrast, such a strong variation in T_R with x is not evident with the heavier rare earths.

Several neutron-diffraction investigations of the Nd ordering in polycrystalline samples of $NdBa_2Cu_3O_{6+x}$ have been reported before now, and have established the main features of the magnetic structures.[15,16] These studies showed that the Nd moments order in a collinear antiferromagnetic structure with ordering wave vector (1/2, 1/2, 1/2), i.e., the direction of the Nd moment alternates in successive unit cells along each crystallographic axis. In optimally doped, superconducting samples ($x \approx 0.95$) the saturated Nd moment was reported to have a magnitude of $\sim 1\mu_B$ and to point along the c direction, while in reduced, nonsuperconducting samples ($x \approx 0.1$) the ordered moment was reported to be slightly smaller and to point in a direction $\sim 45°$ away from the c axis.[15] In samples with intermediate oxygen content the ordering is not well correlated in the c direction, causing a c-axis broadening of the diffraction peaks.[15]

The neutron-diffraction study reported here differs from the previous ones in our use of single-crystal samples. Magnetic diffraction intensities can be measured to a much higher precision with single crystals than with powder samples, and this is important because one way to detect Nd-Cu coupling is to look for small changes in the magnetic peak intensities. Single crystals also have the advantage over powders in that the diffraction peaks are more clearly separated from one another, and together with the better signal to background ratio this means that more diffraction peaks can be measured. Hence, a secondary aim of this work was to obtain a more accurate refinement of the Nd magnetic structure in $NdBa_2Cu_3O_{6+x}$, and to study the effects of different Cu spin orderings on the Nd magnetism. We have already reported on the Cu ordering behavior in oxygen-deficient $NdBa_2Cu_3O_{6+x}$ crystals with different dopants,[17] and the present study is an extension of that work.

II. CRYSTAL PREPARATION AND CHARACTERIZATION

We studied the Nd ordering in three $NdBa_2Cu_3O_{6+x}$ crystals, which we label S (superconducting), and $NS(A)$ and (B) (both nonsuperconducting). The masses of the crystals were 42, 19, and 23 mg, respectively. $NS(A)$ is one of the crystals that we used in our previous study of the Cu magnetic ordering[17] (where we referred to it as $NdBa_2Cu_3O_{6.09}$). These crystals were prepared from a BaO/CuO flux by the slow-cooling method, similar to that described in Refs. 18. The procedure was typically as follows. High-purity (better than 99.99%) Nd_2O_3, $BaCO_3$, and CuO powders were used. Crystal growth took place in 60–70 mbar air as the temperature was decreased from 1020 to ~970 °C at rates of 0.4–0.8 °C per hour. At this point the flux was poured off, and the furnace was evacuated and cooled to room temperature. For crystal $NS(B)$, the cooling to room temperature was slower and the oxygen partial pressure during this cooling higher than for the other crystals. These conditions are expected to favor the spinodal decomposition of the 123 phase with small amounts of Nd replacing Ba on the Ba site. This process cannot be detected by EPMA analysis (see below) because the overall chemical composition remains unchanged.

TABLE I. EPMA analysis of the impurity content and cation ratios for the crystals used in this study. The numbers given are the ratios of each element normalized so that Cu is exactly 3.

Element	$NS(A)$	$NS(B)$	S
Nd	1.01 ± 0.01	0.98 ± 0.02	0.97 ± 0.01
Ba	2.01 ± 0.02	2.03 ± 0.02	2.00 ± 0.01
Cu	3	3	3
Y		0.010 ± 0.006	0.007 ± 0.004
Sn	~0.001		
Al	0.02 ± 0.01		
Zn	~0.001		

The chemical purity of crystals grown this way is usually determined by the crucible type and by the purity of the starting materials. Yttria-stabilized zirconia crucibles were used in the growth of crystals $NS(B)$ and S, and a SnO_2 crucible for $NS(A)$. Corrosion of these crucibles is not a serious problem, but very small amounts of Y [$NS(B)$ and S] or Sn [$NS(A)$] were incorporated into the crystals. In crystal $NS(A)$ some additional contamination was introduced from a slightly impure CuO source material (purity ~99%).

To provide a quantitative assessment of the impurity content we examined each crystal by electron-probe microanalysis (EPMA). The observed cation ratios are listed in Table I. To within experimental error the crystals are stoichiometric in the cations. The amount of Y in crystals $NS(B)$ and S is approximately 1% of the amount of Nd, and no other impurities were found in these crystals. Crystal $NS(A)$ contained trace amounts of Sn and Zn at the limits of detection, and a slightly higher concentration of Al (0.5–1% of Cu) which we believe was introduced from the CuO starting chemical.

Post-growth annealing of the crystals was carried out as follows. Crystal S was annealed in 1 bar oxygen between temperatures of 601 and 379 °C for 790 h. This treatment transformed crystal S into a superconductor with onset transition temperature $T_c = 95.5$ K and width ΔT_c (10–90%) of 0.8 K measured by ac susceptibility. From this T_c value and the oxidation treatment we conclude that the oxygen content x of crystal S is close to 0.97.[19]

Crystal $NS(A)$ was reduced in a gas volumetric system.[20] The crystal was contained inside a small volume together with approximately 5 g of YBCO powder to act as a buffer. The sample space and surrounding volume were separately evacuated, then connected together and heated to 700 °C. Oxygen which degassed from the buffer and crystal was pumped off several times during the course of 2 days. Finally, the system was allowed to equilibrate at 0.5 mbar pressure and cooled down to 200 °C over 10 h. The buffer keeps

the oxygen content of the crystal essentially constant during the cooling. A subsequent refinement of the crystal structure of $NS(A)$ from neutron four-circle diffraction data revealed the oxygen content to be $x=0.09$.[17]

The reduction of crystal $NS(B)$ was carried out at a temperature of 695 °C in an oxygen atmosphere of 0.02 mbar for 138 h. We did not determine the oxygen composition directly, but with these reduction conditions we expect it to be close to $x=0.15$.[19]

III. NEUTRON-DIFFRACTION EXPERIMENTS

Neutron-diffraction measurements were made on the TAS 1 triple-axis spectrometer at the DR3 reactor at Risø National Laboratory. The crystals were wrapped in copper foil and fastened to a copper rod on the end of an Oxford Instruments Heliox insert. The Heliox operates inside a ^{4}He bath cryostat, and can attain a base temperature of 0.30 K by means of a ^{3}He sorption pump system. Neutrons of wavelength 0.24 nm (energy 14.1 meV) were used, selected by Bragg reflection from a pyrolytic graphite monochromator. A graphite filter was placed before the sample to suppress higher-order wavelengths. The spectrometer was employed in three-axis mode with a pyrolytic graphite analyzer set to the elastic condition. Use of the analyzer reduced the count rate, but improved the signal to background ratio. The crystals were aligned with a $[1\bar{1}0]$ direction vertical, so that (hhl) reciprocal-lattice vectors were accessible in the horizontal scattering plane. Slit collimators were installed to define the in-plane divergence of the beam as follows: 60′-monochromator-30′-sample-60′-analyzer-detector.

The method used for deducing the magnetic structures from the neutron Bragg diffraction intensities was the same as that described by Longmore *et al.*[21] Step scans were performed through the Bragg peaks either by rotation of the crystal about the vertical axis at fixed scattering angle 2θ (ω scans), or by variation of ω and 2θ in combination such that the change in scattering vector makes a linear scan parallel to a symmetry direction in reciprocal space [usually $(hh0)$ or $(00l)$]. The area under the measured peak was then multiplied by the Lorentz factor for the scan type, and normalized to the number of counts in the incident beam monitor. The Lorentz factor correction included the sample mosaic and the contribution from the resolution of the spectrometer.[21]

From neutron-scattering theory the magnetic Bragg peak intensities obtained this way are proportional to the function[22]

$$I(\mathbf{Q})=\sum_{\alpha\beta}\langle(\delta_{\alpha\beta}-\hat{Q}_\alpha\hat{Q}_\beta)F^\alpha(\mathbf{Q})F^{\beta*}(\mathbf{Q})\rangle \quad (\alpha,\beta=x,yz), \tag{1}$$

where $\langle\,\rangle$ denotes an average over all equivalent magnetic domains (assumed here to be equally populated), $\delta_{\alpha\beta}$ is the Kronecker delta, $\hat{Q}_\alpha$ is the α component of the unit scattering vector $\hat{\mathbf{Q}}$, and $F^\alpha(\mathbf{Q})$ is the α component of the magnetic structure factor, given in the dipole approximation by

$$F^\alpha(\mathbf{Q})=\sum_j \mu_j^\alpha f_j(\mathbf{Q})\exp(i\mathbf{Q}\cdot\mathbf{r}_j). \tag{2}$$

The sum in Eq. (2) is over all ordered moments in a magnetic unit cell, μ_j^α is the α component of the jth ordered moment, $f_j(\mathbf{Q})$ is the dipole form factor, and $\mathbf{r}_j$ is the displacement of that moment from the origin.

In order to express the observed magnetic diffraction in absolute units we measured a set of crystallographic Bragg peaks. These, together with the known crystal structure of $NdBa_2Cu_3O_{6+x}$ and the standard formulas for the neutron cross sections for nuclear and magnetic scattering, were then used to convert the observed magnetic intensities into the function $I(\mathbf{Q})$ defined in Eqs. (1) and (2) with units of μ_B^2. For convenience we evaluate $I(\mathbf{Q})$ with reference to a magnetic unit cell which corresponds to $2\times2\times2$ crystallographic unit cells. In calculating the magnetic-scattering amplitudes we used magnetic form factors appropriate to each ion. The Cu spins were assumed to be in $3d_{x^2-y^2}$ orbitals with axis of quantization parallel to the crystallographic c axis.[23] For the Nd moments the form factor was taken to be the dipole form factor for the $4f$ electrons in a free Nd^{3+} ion.[24]

IV. RESULTS

As expected, Nd magnetic ordering was observed in all three $NdBa_2Cu_3O_{6+x}$ crystals, while Cu antiferromagnetism was found only in the nonsuperconducting crystals, $NS(A)$ and $NS(B)$. We will begin with these latter two crystals, describing first the Cu magnetic behavior as a function of temperature, and then the phase at low temperatures where Nd and Cu magnetic ordering coexists. Finally we will present the results for the Nd ordering in the superconducting crystal (S).

The general features of the Cu magnetic ordering of oxygen-deficient $NdBa_2Cu_3O_{6+x}$ crystals were reported in our previous paper.[17] The two main conclusions of that study were, (i) that high-purity crystals with stoichiometric cation ratios exhibit only one type of antiferromagnetic ordering of the Cu spins (the AFI phase), and (ii) that doping with excess Nd ions on the Ba site in otherwise chemically pure and stoichiometric crystals destabilizes the AFI phase at low temperatures, causing a reorientation of the Cu magnetic structure which proceeds via a noncollinear turn-angle phase into a second antiferromagnetic structure, the AFII phase. The AFI and AFII phases are distinguishable experimentally by the types of neutron-diffraction peaks observed: the AFI ordering gives rise to peaks with indices $(h+1/2,\ k+1/2,\ l)$ referred to the crystallographic unit cell (h, k, and l are integers), whereas the peaks from the AFII ordering are of the form $(h+1/2,\ k+1/2,\ l+1/2)$. Both sets of peaks are present during the reorientation. The underlying spin structures differ in the stacking sequence along the c direction. In the AFI phase, the spins on the Cu(2) sites within the CuO_2 layers align antiparallel to their nearest neighbors along all three crystallographic axes, and there is no ordered moment on the Cu(1) site in the basal plane. As there are two CuO_2 layers per unit cell this ordering has the same period as the crystal lattice in the c direction, but double the periodicity in the a

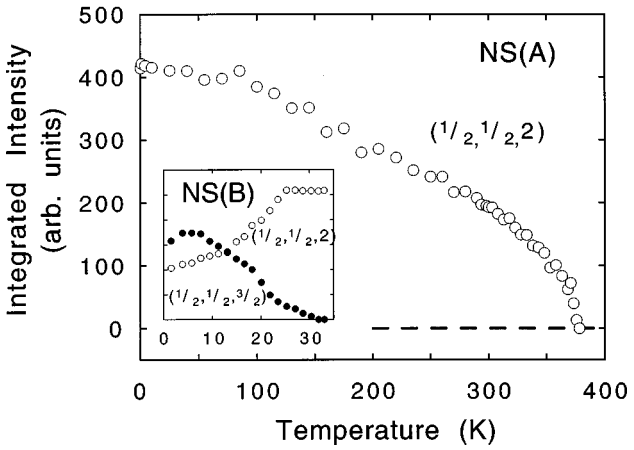

FIG. 1. Integrated intensity of the (1/2,1/2,2) magnetic Bragg peak from the AFI Cu ordering of the $NdBa_2Cu_3O_{6.09}$ crystal $NS(A)$ as a function of temperature. The inset shows the decrease in the peak intensity of the (1/2,1/2,2) and corresponding increase in the peak intensity of the (1/2,1/2,3/2) signifying the onset of the transition to the AFII phase in the $NdBa_2Cu_3O_{6+x}$ crystal $NS(B)$.

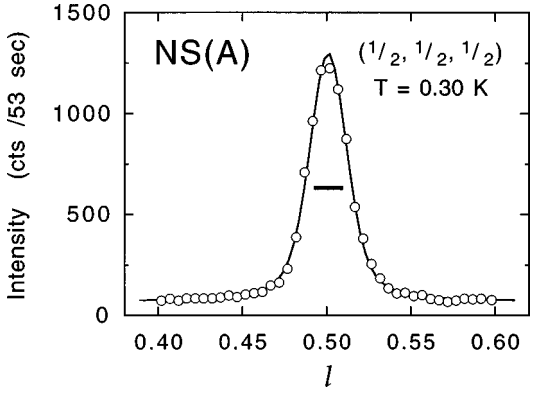

FIG. 2. L scan through the (1/2,1/2,1/2) peak from the Nd ordering in crystal $NS(A)$, showing the slight broadening along the c direction. The instrumental resolution width indicated by the horizontal bar on the figure includes the effect of mosaic, and is estimated from the c-axis widths of the $(1/2,1/2,l)$ series of Cu AFI peaks which are assumed to be resolution limited. The curve is a fit obtained by convolution of the Gaussian resolution function with a Lorentzian intrinsic peak shape.

and b directions. In the AFII phase, the in-plane order is unaffected, but along the c direction the alignment of neighboring Cu(2) spins alternates between parallel and antiparallel, the parallel spins being either side of the basal plane. An ordered moment on the Cu(1) site is now allowed by symmetry, but is not usually observed. This stacking produces a magnetic periodicity parallel to c twice that of the crystal lattice.

Both of the nonsuperconducting crystals used in this study exhibited the AFI phase over a wide range of temperatures below the ordering temperature of $T_N = 378 \pm 1$ K (the same for both crystals), but whereas crystal $NS(A)$ remained in the AFI phase down to the lowest attainable temperature (0.3 K), crystal $NS(B)$ exhibited the AFI-AFII reordering transition below $T_2 \approx 30$ K. These behaviors are illustrated in Fig. 1, the main frame of which shows the integrated intensity of the (1/2,1/2,2) reflection of crystal $NS(A)$ from 0 to T_N, and the inset the (1/2,1/2,2) and (1/2,1/2,3/2) reflections of crystal $NS(B)$ below 35 K. For $NS(B)$, the reduction in intensity at (1/2,1/2,2) and corresponding increase at (1/2,1/2,3/2) reflect the progress of the AFI-AFII reordering as temperature decreases, but the pure AFII phase is not attained even at the lowest temperature.

The onset of Nd magnetic ordering was signaled by the appearance of extra scattering at low temperatures. In the case of crystal $NS(A)$, new peaks of the form $(h+1/2, k+1/2, l+1/2)$ emerged when the temperature was lowered below $T_{Nd} \approx 1.8$ K. These new peaks appear at the same positions in reciprocal space as the Cu AFII phase peaks, but AFI-AFII reordering can be excluded in this case because the observed peak intensities, listed in Table II, do not have the characteristic sinusoidal modulation with l associated with the bilayer. In addition, the temperature below which the new peaks are observed matches closely the Nd ordering temperatures reported from powder neutron diffraction and bulk measurements.[15,16] Figure 2 shows an l scan through one of these new peaks, the (1/2,1/2,1/2), measured at 0.30 K. The peak is broader than the resolution width, and a fit to a Lorentzian intrinsic peak shape convolved with the Gaussian resolution function established an intrinsic width [half width at half maximum (HWHM)] of 0.053 nm^{-1}, corresponding to a correlation length $\xi_c \approx 19$ nm. There was no variation in ξ_c with temperature within error. The peak was resolution limited in scans parallel to $(h,h,0)$. Figure 3(a) shows the temperature dependence of the intensity of the (1/2,1/2,1/2) scan integrated over l. The line is a power law of the form $I_0(1-T/T_{Nd})^{2\beta}$ fitted to the data in the range $1.2\,\mathrm{K} \leqslant T \leqslant 1.8\,\mathrm{K}$, from which we estimate the order parameter critical exponent β to be 0.39 ± 0.05, and $T_{Nd} = (1.77 \pm 0.03)$ K.

By contrast, no sharp Bragg peaks showed up below T_{Nd} in the neutron scattering from crystal $NS(B)$. We did, however, observe extra scattering in the form of a diffuse ridge running parallel to $(0,0,l)$ in reciprocal space, passing through (1/2,1/2,0). The ridge was resolution limited in scans parallel to $(h,h,0)$, and its intensity varied only weakly over the experimentally measured range $-2 \leqslant l \leqslant 6.5$. This implies a highly two-dimensional state of magnetic ordering in which the Nd moments are ordered antiferromagnetically over a long range within the ab planes, but are practically uncorrelated in the c direction. The temperature dependence of the scattering at the point (1/2,1/2,1.3) on the ridge is shown in Fig. 3(b). The possibility of determining a critical exponent is precluded by the experimental scatter, but we have the impression that the initial rate of increase in the ridge amplitude below T_{Nd} is less than the intensity of the Nd ordering of crystal $NS(A)$ in Fig. 3(a).

Having identified the scattering associated with the Nd magnetic ordering we now turn to the issue of magnetic coupling between the Nd and Cu sublattices. We searched for this in crystal $NS(A)$, employing two distinct tests. Firstly, we compared the integrated intensities of the set of six $(1/2, 1/2, l)$ AFI Cu magnetic Bragg peaks, $1 \leqslant l \leqslant 6$, at temperatures of 4.2 and 0.3 K. The ratios of the intensities measured at the two temperatures are shown in Fig. 4. To within experimental error the ratios do not deviate from unity, and this

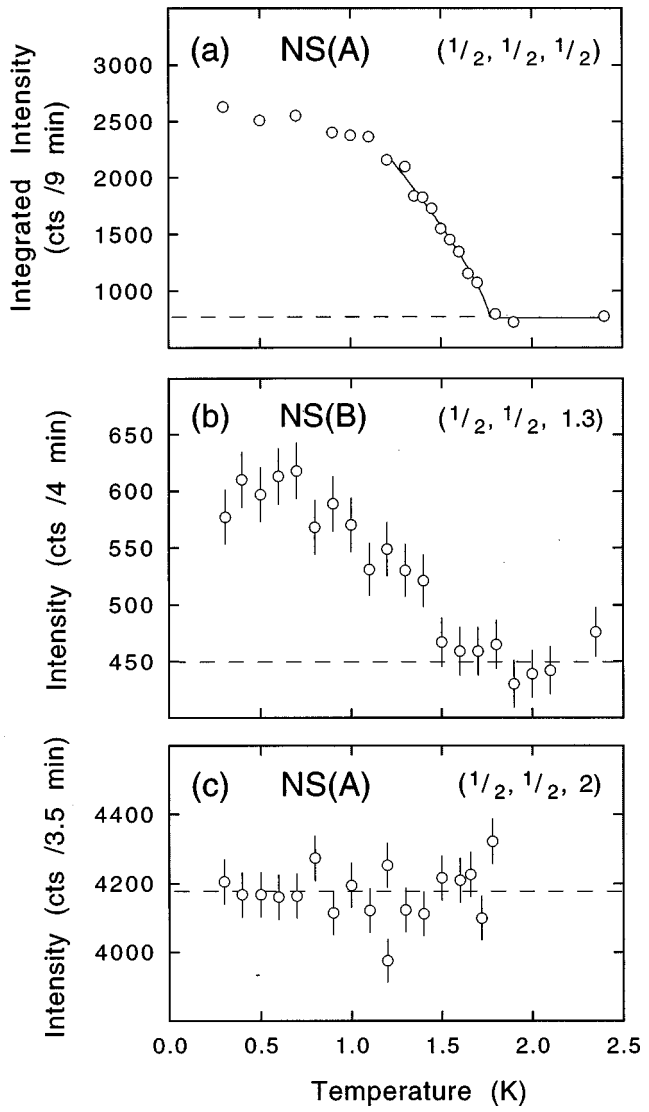

FIG. 3. (a) Temperature dependence of the *l*-integrated intensity of the (1/2,1/2,1/2) magnetic reflection (including background) arising from the Nd magnetic ordering in crystal $NS(A)$. The line is a power law corresponding to an order-parameter critical exponent $\beta=0.39$ and $T_{\mathrm{Nd}}=1.77$ K. (b) Intensity at the point (1/2,1/2,1.3) on the ridge of diffuse scattering observed in crystal $NS(B)$. The similarity with the temperature variation shown in (a) is evidence that the scattering is from a two-dimensional ordering of the Nd spins. (c) Peak intensity of the (1/2,1/2,2) antiferromagnetic Bragg peak from the AFI ordering of the Cu sublattice in crystal $NS(A)$. The absence of any detectable change in the (1/2,1/2,2) intensity as the Nd ordering develops allows us to put an upper limit on the size of any Nd-Cu magnetic coupling.

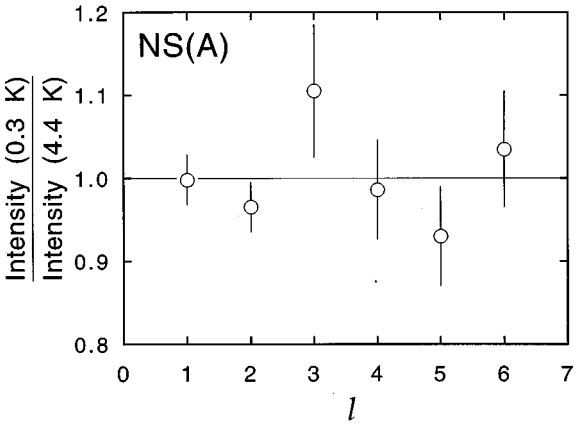

FIG. 4. The ratio of the integrated intensities of the $(1/2,1/2,l)$ magnetic peaks from crystal $NS(A)$ measured t temperatures of 3.3 and 4.4 K. This set of peaks arises from the AFI Cu spin ordering, and the absence of any systematic temperature variation is evidence that there is no change in the Cu spin structure on cooling below the Nd magnetic ordering transition.

is an indication that any change in the Cu spin structure in response to the Nd ordering is very small. Second, we aligned the spectrometer on the maximum of the (1/2,1/2,2) Cu magnetic Bragg peak and scanned the temperature stepwise from 0.3 to 2 K, counting for a preset monitor value (duration approximately 3.5 min) at each temperature. The scan is shown in Fig. 3(c), and is seen to be independent of temperature within the limits of experimental error. The (1/2, 1/2,2) reflection is close to the optimum constructive interference condition for diffraction from the AFI spin structure, and so almost any conceivable change in the magnetic ordering of the Cu sublattice would cause a reduction in intensity at (1/2,1/2,2). We judge from the entirety of measurements shown in Fig. 3(c) and 4 that any such change on passing through T_{Nd} must be smaller than 1% of the peak intensity.

The implication from the preceding results is that the magnetic ordering on the Nd and Cu sublattices is independent of one another to within the limits of detection. This means that the additional scattering observed at temperatures below T_{Nd} can be ascribed to magnetic ordering of the Nd sublattice alone, and by modeling this scattering we can refine the magnetic structure of the Nd moments. In Table II we have listed the intrinsic intensities of the accessible $(h+1/2,k+1/2,l+1/2)$ reflections measured from crystal $NS(A)$ at 0.3 K, and alongside these are the calculated intensities from the model that gave the best agreement according to the least-squares criterion. The only variable parameters in the fitting were the angle of the Nd moment from the *c* axis θ_{Nd}, and the magnitude of the ordered Nd moment μ_{Nd}. The refined values of these parameters were $\theta_{\mathrm{Nd}}=90°\pm5°$, and $\mu_{\mathrm{Nd}}=1.58\pm0.03\mu_B$. To within the error, therefore, the Nd moment is found to lie in the *ab* plane. Nothing can be deduced about the in-plane orientation of the ordered moment because in calculating the intensities we averaged over all equivalent magnetic domains in tetragonal symmetry. The refined Nd magnetic structure for crystal $NS(A)$ is illustrated in Fig. 5(a).

We carried out a similar refinement for crystal $NS(B)$, except that because the ordering was essentially two-dimensional the procedure described in Ref. 21 was adopted. Scans made perpendicular to the scattering ridge at several values of l were scaled by Lorentz factors for a two-dimensional system derived from the Cooper-Nathans resolution function, and the resulting intensities were compared with calculations for a two-dimensional magnetic structure. In Table III we give the observed and calculated intensities for the case when $\theta_{\mathrm{Nd}}=90°$ as found for the Nd ordered moment in crystal $NS(A)$. The refined ordered moment for

TABLE II. Observed and calculated integrated intensities of the magnetic reflections from the Nd magnetic structure at 0.3 K for crystal $NS(A)$ (nonsuperconducting $NdBa_2Cu_3O_{6+x}$, $x=0.09$). The best fit model has an ordered moment of magnitude $\mu_{Nd}=1.58\mu_B$ at an angle $\theta_{Nd}=90°$ to the c axis. The observed intensities have been corrected for the Lorentz factor. The errors indicated are the statistical uncertainties, but there is also an overall uncertainty in the calibration of the absolute intensity of approximately 10%.

(h,k,l)	I_{obs} (μ_B^2)	I_{calc} (μ_B^2)
$(\frac{1}{2},\frac{1}{2},\frac{1}{2})$	64±3	80
$(\frac{1}{2},\frac{1}{2},\frac{3}{2})$	95±3	99
$(\frac{1}{2},\frac{1}{2},\frac{5}{2})$	111±3	114
$(\frac{1}{2},\frac{1}{2},\frac{7}{2})$	121±5	118
$(\frac{1}{2},\frac{1}{2},\frac{9}{2})$	123±3	115
$(\frac{1}{2},\frac{1}{2},\frac{11}{2})$	120±4	108
$(\frac{1}{2},\frac{1}{2},\frac{13}{2})$	100±4	99
$(\frac{3}{2},\frac{3}{2},\frac{1}{2})$	47±5	55
$(\frac{3}{2},\frac{3}{2},\frac{3}{2})$	55±5	56
$(\frac{3}{2},\frac{3}{2},\frac{5}{2})$	67±5	58
		$\chi^2=6.1$

this fit is $\mu_{Nd}=1.2\pm0.1\mu_B$. Although the agreement is acceptable, reasonable fits can also be achieved with θ_{Nd} anywhere in the range 50°–90°.

Finally, we will briefly describe the Nd magnetic ordering observed in crystal S, the superconducting crystal. Scans through the $(h+1/2,k+1/2,l)$ positions in reciprocal space did not contain any peaks at any temperature, and this confirmed the absence of long-range magnetic order of the Cu spins. Peaks centered at $(h+1/2,k+1/2,l+1/2)$ developed

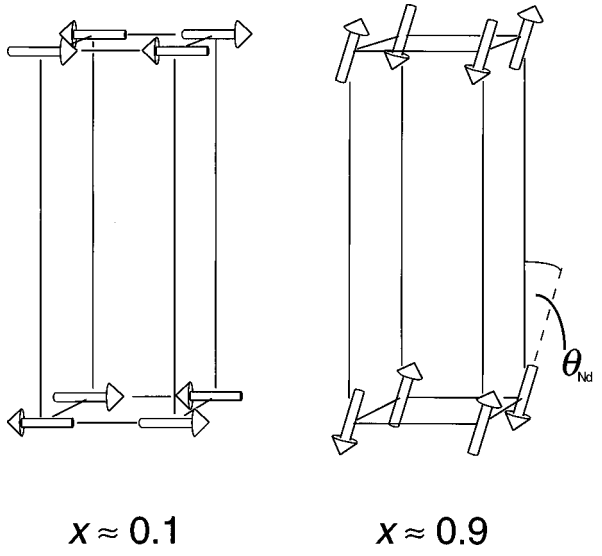

FIG. 5. The ordered magnetic arrangements found for the Nd moments in $NdBa_2Cu_3O_{6+x}$ crystals $NS(A)$ ($x\approx0.1$) and S($x\approx0.9$). Only the Nd moments are shown. θ_{Nd} is the tilt of the spin axis from the c direction, and is found to be $12°\pm12°$ for crystal S.

TABLE III. Observed and calculated integrated intensities for scans across the diffuse scattering ridge from the two-dimensional Nd magnetic ordering at 0.3 K observed in crystal $NS(B)$. The calculated intensities are for an ordered moment of magnitude $\mu_{Nd}=1.2\mu_B$ at an angle $\theta_{Nd}=90°$ to the c axis. The observed intensities have been corrected for the two-dimensional Lorentz factor.

(h,k,l)	I_{obs} (μ_B^2)	I_{calc} (μ_B^2)
$(\frac{1}{2},\frac{1}{2},0)$	9±3	10
$(\frac{1}{2},\frac{1}{2},1.75)$	19±3	14
$(\frac{1}{2},\frac{1}{2},3.25)$	15±2	16
$(\frac{1}{2},\frac{1}{2},6.65)$	7±3	13
		$\chi^2=3$

below $T_{Nd}=0.62$ K corresponding to magnetic ordering of the Nd sublattice in the same mode as was found for the stoichiometric nonsuperconducting crystal $NS(A)$. The Nd magnetic peaks were almost resolution limited in scans parallel to $(0,0,l)$, but tails just visible at the base of the peaks indicated a slight intrinsic broadening. We estimate the intrinsic width (HWHM) to be roughly 0.01 nm^{-1}, corresponding to a correlation length $\xi_c\sim100$ nm. Figure 6 shows the temperature dependence of the intensity of the (1/2,1/2,1/2) peak integrated over l. The decrease in intensity as the temperature approaches T_{Nd} is more rapid than for crystal $NS(A)$ [Fig. 3(a)], and this is reflected in a significantly smaller value of the order-parameter critical exponent obtained from a power-law fit over the temperature range $0.46<T<0.68$ K: $\beta=0.23\pm0.01$, and $T_{Nd}=(0.62\pm0.01)$ K. Table IV lists the observed magnetic Bragg peak intensities, and alongside these are the calculated values obtained from the parameters of the best-fit model: $\theta_{Nd}=12°\pm2°$ and $\mu_{Nd}=1.40\pm0.02\mu_B$. The Nd moments are nearly parallel to the c direction in the ordered phase, as depicted in Fig. 5(b). We believe that the small tilt suggested by the fit is

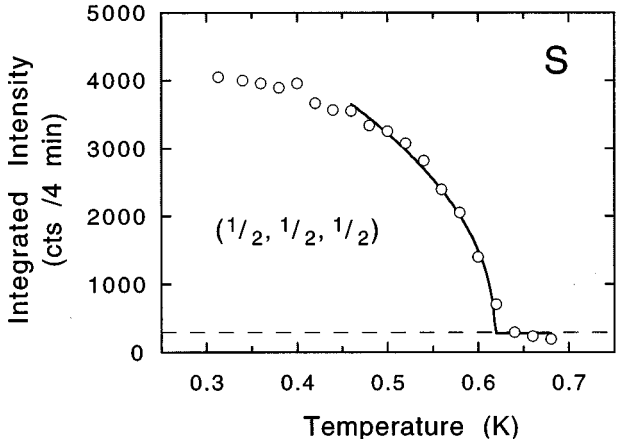

FIG. 6. Temperature variation of the integrated intensity of the (1/2,1/2,1/2) magnetic reflection corresponding to the development of Nd magnetic ordering in superconducting $NdBa_2Cu_3O_{6+x}$ crystal S. The line is a power law corresponding to an order-parameter critical exponent $\beta=0.23$ and $T_{Nd}=0.62$ K.

TABLE IV. Observed and calculated integrated intensities of the magnetic reflections from the Nd magnetic structure at 0.3 K for crystal *S* (superconducting $NdBa_2Cu_3O_{6+x}$). The best fit model has an ordered moment of magnitude $\mu_{Nd}=1.40\mu_B$ at an angle $\theta_{Nd}=12°$ to the *c* axis. The observed intensities have been corrected for the Lorentz factor. The errors indicated are the statistical uncertainties, but there is also an overall uncertainty in the calibration of the absolute intensity of approximately 10%.

(h,k,l)	I_{obs} (μ_B^2)	I_{calc} (μ_B^2)
$(\frac{1}{2},\frac{1}{2},\frac{1}{2})$	115±4	111
$(\frac{1}{2},\frac{1}{2},\frac{3}{2})$	84±3	78
$(\frac{1}{2},\frac{1}{2},\frac{5}{2})$	50±1	49
$(\frac{1}{2},\frac{1}{2},\frac{7}{2})$	29±1	32
$(\frac{1}{2},\frac{1}{2},\frac{9}{2})$	22±2	21
$(\frac{1}{2},\frac{1}{2},\frac{11}{2})$	15±1	15
$(\frac{1}{2},\frac{1}{2},\frac{13}{2})$	12±1	11
$(\frac{3}{2},\frac{3}{2},\frac{1}{2})$	77±8	83
$(\frac{3}{2},\frac{3}{2},\frac{3}{2})$	65±7	77
$(\frac{3}{2},\frac{3}{2},\frac{5}{2})$	59±5	69
$(\frac{3}{2},\frac{3}{2},\frac{7}{2})$	51±5	58
		$\chi^2=2.7$

statistically significant because the value of χ^2 increases from 2.7 to 4.9 if θ_{Nd} is fixed at 0°.

V. DISCUSSION AND CONCLUSIONS

In a sense, the central result of this study is a null one: we were unable to observe any Nd-Cu magnetic coupling. This finding contrasts with the case of nonsuperconducting $PrBa_2Cu_3O_{6+x}$ in which Pr-Cu coupling is responsible for the noncollinear AFIII magnetic ordering observed at temperatures below T_{Pr}. If there is any tendency for the Nd and Cu spins to form the AFIII phase below T_{Nd} then the 1% upper limit we have established on any anomaly in the Cu magnetic peak intensity at T_{Nd} in crystal $NS(A)$ constrains the Cu spin turn angle ϕ_{Cu} to be less than $\cos^{-1}(\sqrt{0.99})=6°$. An estimate of the maximum Nd-Cu pseudodipolar interaction energy can then be made from the energy required for two antiparallel Cu spins on adjacent layers in the bilayer, coupled by an exchange energy $J_{\perp 1}\approx 10\,\text{meV}$,[25] to counterrotate through angles $\pm\phi_{Cu}$: $J_{\perp 1}S_{Cu}^2[1-\cos(2\phi_{Cu})]\approx 0.05\,\text{meV}$, some 20 times less than that found for $PrBa_2Cu_3O_{6+x}$.[7] As the ionic radius decreases across the trivalent rare-earth series, any *R*-Cu coupling in the other superconducting members of the $RBa_2Cu_3O_{6+x}$ family should be even weaker.

This constraint on the pseudodipolar coupling strength might be compared with the (diagonal) exchange coupling derived from measurements of the relaxation of the crystal-field excitations. Aksenov and Kabanov[26] have calculated the linewidth of the $\Gamma_3-\Gamma_4$ crystal-field transition of Tm^{3+} in $Tm_{0.1}Y_{0.9}Ba_2Cu_3O_{6+x}$ assuming that the relaxation is due to Cu antiferromagnetic spin fluctuations, and that the Tm-Cu coupling is only through the diagonal elements in the exchange tensor. They needed a coupling strength of ~5 meV to match their calculations to the experimental data.[3] This is two orders of magnitude larger than the upper limit we have placed on the pseudodipolar coupling. As discussed in the introduction, the diagonal terms couple preferentially to the $\mathbf{q}=(0,0)$ fluctuations while the off-diagonal (pseudodipolar) terms couple preferentially to the strongly enhanced (by more than two orders of magnitude according to some models[27]) fluctuations in the vicinity $\mathbf{q}=(\pi/a,\pi/b)$, and so even a rather small pseudodipolar coupling could transmit a significant relaxation effect to the *R* site. We cannot determine from this analysis, therefore, which terms in the exchange tensor are most important in mediating the *R*-Cu interaction that causes relaxation to local excitations of the *R* ion. It would be very interesting in this respect to repeat the calculations of Ref. 26 for a pseudodipolar coupling, to ascertain what strength of pseudodipolar interaction would be needed to describe the experimental relaxation data.

The magnetic structures that we have determined for stoichiometric $NdBa_2Cu_3O_{6+x}$ with crystals $NS(A)$ and *S* are largely similar to what have been proposed before from neutron-diffraction measurements on polycrystalline samples, but differ in respect of the magnitude and direction of the ordered Nd moments. In $NdBa_2Cu_3O_{6.09}$, crystal $NS(A)$, we find a Nd ordered moment of $\mu_{Nd}=1.58\pm 0.03\mu_B$ oriented in some direction in the *ab* plane ($\theta_{Nd}\approx 90°$), compared with $\mu_{Nd}=0.85\pm 0.04\mu_B$ and $\theta_{Nd}\approx 45°$ deduced by Clinton *et al.*[15] The anisotropy in the measured magnetic susceptibility at low temperatures,[28] and calculations from models for the crystalline electric field[29] both indicate an easy direction for the Nd moment in the *ab* plane, consistent with our findings. The discrepancies between our model for oxygen-deficient $NdBa_2Cu_3O_{6+x}$, and that of Ref. 15 may be a result of the limited number and accuracy of the magnetic Bragg peaks measured in the powder-diffraction study. We have already emphasized the advantages of using single crystals over polycrystalline samples for magnetic structure determination earlier on in this paper.

For the superconducting $NdBa_2Cu_3O_{6+x}$, crystal we find that the ordered Nd moment is tilted 12° away from the *c* direction, in near agreement with Clinton *et al.*[15] who concluded the moment direction to be actually along *c*. Our value of $1.40\pm 0.02\mu_B$ for μ_{Nd} is a little larger than the values reported previously: $1.07\pm 0.07\mu_B$ and $1.14\pm 0.06\mu_B$.[16] In addition, it is interesting that we find the ordered moment to be largest in the crystal with least oxygen, whereas Ref. 15 reports the reverse trend.

The switch in the direction of the ordered moment from perpendicular to nearly parallel to the *c* axis with increasing oxygen content is in line with the single ion anisotropy deduced by Allenspach *et al.* from neutron inelastic-scattering data.[29] This agreement confirms that the direction of the ordered moment is determined primarily by the local crystalline electric field at the Nd site.

It is less clear how to interpret the magnetic structure data on crystal $NS(B)$. It will be recalled that this sample may contain some excess Nd on the Ba site, and that the Cu sublattice is in the transitional turn-angle state between the AFI and AFII magnetic structures. We have speculated before[17] that one effect of having Nd ions on the Ba site is to

generate free Cu^{2+} spins in the basal plane, and that this adds an effective ferromagnetic coupling along the *c* direction causing the AFI-AFII reorientation.[30] The same mechanism could explain the lack of magnetic coherence along the *c* direction in the Nd ordering of crystal $NS(B)$. In stoichiometric $NdBa_2Cu_3O_{6+x}$ the *c*-axis coupling between adjacent Nd spins is antiferromagnetic, as shown by the results of crystal $NS(A)$, but any interaction with free spins situated in the basal plane would tend to add a ferromagnetic contribution to the *c*-axis coupling.[30] Hence, the observed two-dimensional magnetic ordering of the Nd sublattice could be the result of competing ferro- and antiferromagnetic interactions along *c*. It is also possible, however, that the Nd ions on the Ba sites carry a paramagnetic moment which could provide an alternative source of frustration to explain the two-dimensional ordering. Polycrystalline samples with intermediate oxygen contents have also been found to exhibit two-dimensional Nd magnetic ordering,[15,29] but this behavior occurs only when $x>0.3$ and so is unlikely to be caused by the same mechanism as applies in crystal $NS(B)$, for which $x\approx 0.15$. Experiments with crystals that have no Nd ions on the Ba site, but that exhibit the AFI-AFII intermediate phase due to basal plane substituents such as Al could be informative in establishing the dominant source of frustration in the Nd ordering.

ACKNOWLEDGMENTS

The neutron-scattering experiments were supported by the EC TMR-Access to Large Scale Facilities Program at Risø National Laboratory. A.T.B. thanks the Condensed Matter Physics and Chemistry Department at Risø for hospitality during an extended visit in 1998.

[1] J. T. Markert, Y. Dalichaouch, and M. B. Maple, in *Physical Properties of High Temperature Superconductors I*, edited by D. M. Ginsberg (World Scientific, Singapore, 1989), Chap. 6; J. W. Lynn, in *High Temperature Superconductors*, edited by J. W. Lynn (Springer-Verlag, New York, 1990), Chap. 8.

[2] An early review of the properties of $PrBa_2Cu_3O_{6+x}$ is given by H. B. Radousky, J. Mater. Res. **7**, 1917 (1992).

[3] R. Osborn and E. A. Goremychkin, Physica C **185–189**, 1179 (1991).

[4] A. T. Boothroyd, A. Mukherjee, and A. Murani, Phys. Rev. Lett. **77**, 1600 (1996).

[5] J. A. Hodges, P. Bonville, P. Imbert, and G. Jéhanno, Physica C **184**, 259 (1991); J. A. Hodges, P. Bonville, P. Imbert, G. Jéhanno, and P. Debray, *ibid.* **184**, 270 (1991).

[6] J. T. Markert, T. W. Noh, S. E. Russek, and R. M. Cotts, Solid State Commun. **63**, 847 (1987); H. Alloul, A. Mahajan, H. Casalta, and O. Klein, Phys. Rev. Lett. **70**, 1171 (1993).

[7] A. T. Boothroyd, A. Longmore, N. H. Andersen, E. Brecht, and Th. Wolf, Phys. Rev. Lett. **78**, 130 (1997).

[8] S. Skanthakumar, J. W. Lynn, N. Rosov, G. Cao, and J. E. Crow, Phys. Rev. B **55**, R3406 (1997).

[9] S. Uma, W. Schnelle, E. Gmelin, G. Rangarajan, S. Skanthakumar, J. W. Lynn, R. Walter, T. Lorenz, B. Büchner, E. Walker, and A. Erb, J. Phys.: Condens. Matter **10**, L33 (1998).

[10] Bulk superconductivity has recently been observed in single crystals of $PrBa_2Cu_3O_{6+x}$ grown by the traveling-solvent floating-zone method, Z. Zou, K. Oka, T. Ito, and Y. Nishihara, Jpn. J. Appl. Phys., Part 2 **36**, L18 (1997).

[11] I. Felner, U. Yaron, I. Nowik, E. R. Bauminger, Y. Wolfus, E. R. Yacoby, G. Hilscher, and N. Pillmayr, Phys. Rev. B **40**, 6739 (1989); D. W. Cooke, R. S. Kwok, M. S. Jahan, R. L. Lichti, T. R. Adams, C. Boekema, W. K. Dawson, A. Kebede, J. Schwegler, J. E. Crow, and T. Mihalisin, J. Appl. Phys. **67**, 5061 (1990); A. P. Reyes, D. E. MacLaughlin, M. Takigawa, P. C. Hammel, R. H. Heffner, J. D. Thompson, J. E. Crow, A. Kebede, T. Mihalisin, and J. Schwegler, Phys. Rev. B **42**, 2688 (1990).

[12] A. Kebede, C.-S. Jee, J. Schwegler, J. E. Crow, T. Mihalisin, G. H. Myer, R. E. Salomon, P. Schlottmann, M. V. Kuric, S. H. Bloom, and R. P. Guertin, Phys. Rev. B **40**, 4453 (1989); W.-H. Li, J. W. Lynn, S. Skanthakumar, T. W. Clinton, A. Kebede, C.-S. Jee, J. E. Crow, and T. Mihalisin, *ibid.* **40**, 5300 (1989); G. Wortmann and I. Felner, Solid State Commun. **75**, 981 (1990); A. Kebede, J. P. Rodriquez, I. Perez, T. Mihalisin, G. Myer, J. E. Crow, P. P. Wise, and P. Schlottmann, J. Appl. Phys. **69**, 5376 (1991).

[13] A. T. Boothroyd, Physica B **241–243**, 792 (1998).

[14] R. Sachidanandam, T. Yildirim, A. B. Harris, A. Aharony, and O. Entin-Wohlman, Phys. Rev. B **56**, 260 (1997).

[15] T. W. Clinton, J. W. Lynn, J. Z. Liu, Y. X. Jia, T. J. Goodwin, R. N. Shelton, B. W. Lee, M. Buchgeister, M. B. Maple, and J. L. Peng, Phys. Rev. B **51**, 15 429 (1995).

[16] K. N. Yang, J. M. Ferreira, B. W. Lee, M. B. Maple, W.-H. Li, J. W. Lynn, and R. W. Erwin, Phys. Rev. B **40**, 10 963 (1989); P. Fischer, B. Schmid, P. Brüesch, F. Stucki, and P. Unternährer, Z. Phys. B **74**, 183 (1989).

[17] E. Brecht, P. Schweiss, Th. Wolf, A. T. Boothroyd, J. M. Reynolds, N. H. Andersen, H. Lütgemeier, and W. W. Schmahl, Phys. Rev. B **59**, 3870 (1999).

[18] Th. Wolf, W. Goldacker, B. Obst, G. Roth, and R. Flükiger, J. Cryst. Growth **96**, 1010 (1989); Th. Wolf, A.-C. Bornarel, H. Küpfer, R. Meier-Hirmer, and B. Obst, Phys. Rev. B **56**, 6308 (1997).

[19] T. B. Lindemer, E. D. Specht, P. M. Martin, and M. L. Flitcroft, Physica C **255**, 65 (1995).

[20] N. H. Andersen, B. Lebech, and H. F. Poulsen, Physica C **172**, 31 (1990).

[21] A. Longmore, A. T. Boothroyd, C. Changkang, H. Yongle, M. P. Nutley, N. H. Andersen, H. Casalta, P. Schleger, and A. N. Christensen, Phys. Rev. B **53**, 9382 (1996).

[22] S. W. Lovesey, *Theory of Neutron Scattering from Condensed Matter* (Oxford University Press, Oxford, 1984), Vol 2.

[23] S. Shamoto, M. Sato, J. M. Tranquada, B. J. Sternlieb, and G. Shirane, Phys. Rev. B **48**, 13 817 (1993).

[24] P. J. Brown, in *International Tables for X-Ray Crystallography*, edited by A. J. C. Wilson (Kluwer Academic, Dordrecht, 1992), Vol. C.

[25] D. Reznik, P. Bourges, H. F. Fong, L. P. Regnault, J. Bossy, C. Vettier, D. L. Milius, I. A. Aksay, and B. Keimer, Phys. Rev. B **53**, R14 741 (1996); S. M. Hayden, G. Aeppli, T. G. Perring, H.

A. Mook, and F. Dogan, *ibid.* **54**, R6905 (1996).
[26] V. L. Aksenov and V. V. Kabanov, Phys. Rev. B **49**, 3524 (1994).
[27] A. J. Millis, H. Monien, and D. Pines, Phys. Rev. B **42**, 167 (1990); H. Monien, D. Pines, and M. Takigawa, *ibid.* **43**, 258 (1991).
[28] N. Senthilkumaran, T. Sarkar, G. Rangarajan, C. Chankang, J. W. Hodby, M. Spears, and B. M. Wanklyn, Physica B **223&224**, 565 (1996).
[29] P. Allenspach, J. Mesot, U. Staub, M. Guillaume, A. Furrer, S.-I. Yoo, M. J. Kramer, R. W. McCallum, H. Maletta, H. Blank, H. Mutka, R. Osborn, M. Arai, Z. Bowden, and A. D. Taylor, Z. Phys. B **95**, 301 (1994); P. Allenspach, B. W. Lee, D. A. Gajewski, V. B. Barbeta, M. B. Maple, G. Nieva, S.-I. Yoo, M. J. Kramer, R. W. McCallum, and L. Ben-Dor, Z. Phys. B **96**, 455 (1995).
[30] N. H. Andersen and G. Uimin, Phys. Rev. B **56**, 10 840 (1997).